

NTTC FILE COPY

(4) (circled)

AD-A198 931

Office of the Chief of Naval Research  
Contract N00014-85-0187  
Technical Report No. UWA/DME/TR-88/60

HRR FIELD OF A MOVING CRACK, AN EXPERIMENTAL ANALYSIS

Mahyar S. Dadkhah and Albert S. Kobayashi

September 1988

The research reported in this technical report was made possible through support extended to the Department of Mechanical Engineering, University of Washington, by the Office of Naval Research under Contract N00014-85-K-0187. Reproduction in whole or in part is permitted for any purpose of the United States Government.

Department of Mechanical Engineering  
College of Engineering  
University of Washington

DTIC  
SELECTED  
SEP 16 1988  
S E D

... ..  
... ..  
... ..  
... ..

88 9 15 051

## HRR FIELD OF A MOVING CRACK, AN EXPERIMENTAL ANALYSIS

Mahyar S. Dadkhah and Albert S. Kobayashi  
University of Washington  
Department of Mechanical Engineering  
Seattle, Washington 98195 USA

### ABSTRACT

An improved moire interferometry was used to record simultaneously both the vertical and horizontal displacements associated with stable crack growth in uniaxially and biaxially loaded 2024-0 and 2024-T3 aluminum, single edge notched specimens. For stable crack growth up to 5 mm, the vertical displacement field showed the dominance of the HRR field but the HRR field was detected in the horizontal displacement only at the initial stage of loading. The far and near field J-integrals were path independent and yielded the correct crack tip displacements only at the initial stage of loading in the horizontal direction and at the terminal stage of loading in the vertical displacement field. The preliminary results indicate that J-characterization of a moving crack, including that of rapid propagation, may not be valid for these ductile materials for this specimen configuration. (JFS) ←

### INTRODUCTION

For the past two decades, an enormous amount of research and development efforts have been expended in justifying and quantifying the J-integral values of ductile engineering materials. From the view point of material testing, the J-integral offers an experimental convenience over other proposed ductile fracture criteria, such as crack opening displacement (COD) and crack tip opening displacement (CTOD). This advantage is manifested by the use of far field J-value, which under certain conditions represents the crack tip J-value through Rice's path independence proof [1]. In contrast, the COD and the CTOD pose untold experimental challenges. The asymptotic crack tip solution, which justifies Rice's J-integral, for power hardening materials was later presented by Hutchinson [2] and Rice and Rosengren [3] and is commonly referred to as the HRR field.

The extent of this HRR field has been studied numerically by McMeeking and Parks [4], Shih and German [5] and Shih [6] for a single-edged crack beam under bending and a center crack plate under uniaxial tension. Shih [6] summarizes the findings of these three papers by the following two criteria, in terms of a size requirement, for the J-dominant condition to exist.

For an incompressible fully plastic power hardening material, the uniaxial strain  $\epsilon$  is related to uniaxial stress  $\sigma$  by

$$\frac{\epsilon}{\epsilon_0} = \alpha \left( \frac{\sigma}{\sigma_0} \right)^n \quad (1)$$

For a crack tip field under pure bending, the J integral characterizes the plane-strain crack tip field if

$$b > 25 J/\sigma_0 \quad (2)$$

Likewise condition for a plane strain crack tip field under pure tension is

$$b > 200 J/\sigma_0 \quad (3)$$

Here  $b$  is the characteristic size parameter which is the remaining ligament between the crack tip and the edge of the specimen.  $\epsilon_0$  and  $\sigma_0$  are often referred to as the yield strain and yield stress, respectively where  $\epsilon_0 = \sigma_0/E$  and  $E$  is the modulus of elasticity.  $\alpha$  and  $n$  are experimentally determined parameters for the power hardening law.

Although the path independence of the J-integral is valid only for nonlinear elastic solids or deformation theory of plasticity, Shih [7], through numerical analysis, found that this restriction could be relaxed for small crack extension of the order of 5 mm. To the writers' best knowledge, comparable experimental analysis on the path independence of the J-integral or on the validity of the previously mentioned J-dominance criteria under crack extension does not exist. Chiang et al. [8] has shown that in blunt notched 2024-0 and 6061-T6 aluminum specimens, the HRR zone is restricted to an extremely small strip region, which excludes the region immediately adjacent to the notch tip.

The purpose of this paper is to provide experimental analyses of the above J-dominance criterion and on the path independence of J under small crack extension. Such analyses should provide some insight to the eventual problem of study, namely the crack tip singularity field accompanying a rapidly propagating crack in a ductile material.

#### EXPERIMENTAL PROCEDURE

The vertical and horizontal displacement in uniaxially and biaxially loaded 2024-0 and 2024-T3 aluminum, single-edged notched plate were determined by an improved moire interferometry. Figure 1 shows the specimen configuration which was loaded on a special testing machine [9]. Figures 2a and 2b show the uniaxial stress-strain relations in the vertical direction for the 2024-0 and 2024-T3 aluminum, respectively which were used in this study. Also shown are the two parameters for the corresponding power hardening relations. Similar relations in the horizontal directions were determined for the two aluminum plates and were found to be within 5% of the experimental data shown in Figure 2.

The improved moire interferometry consists of a beam splitter and a prism which records simultaneously the vertical and horizontal displacements in a single frame [10]. This method removes the approximation, which was necessary in previous studies [11, 12], in the J-estimation. It is conducive for high speed photographic recording of the transient moire fringes associated with a rapidly propagating crack. For this study, the moire fringes during stable crack growth were recorded by a motorized Nikon camera.

An AST Turboscan Digitizer and a Macintosh II computer were used to digitize the photographically recorded moire fringes. A software was developed to compute the three strain components from the coded displacement field. These strain components were used to compute the J-integral value along given rectangular contours, which encompass the crack tip, as shown in Figure 1 [13].

## RESULTS

2024-0 and 2024-T3 aluminum specimens were loaded uniaxially, i.e., at a biaxial ratio  $B = 0$ , and biaxially with the horizontal load being twice the vertical load or  $B = 2$ . Table 1 shows the test matrix of this limited study together with the maximum crack extensions achieved in each of the five tests. Figure 3 shows the load versus load-line displacement for a biaxially loaded ( $B = 2$ ) 2024-0 aluminum specimen.

Figures 4a and 4b show typical moire fringes, i.e., the vertical displacement,  $v$ , and the horizontal displacement,  $u$ , for the biaxially loaded 2024-0 aluminum specimen. Also shown are typical integration contours used for the J-integral determination. The J values obtained along these contours are shown in Table 2. Path independence, i.e., within a nine percent scatter in the J-values, is noted. Similar results were noted in the other four tests.

Figures 5 and 6 show typical log-log plots of the  $v$ - and  $u$ -displacement fields obtained from the moire fringes. Also shown are the log-log plots of displacements versus radial distance  $r$  of the linear elastic (LEFM) and HRR fields at a crack tip polar angle of  $\theta = 45^\circ$ . The HRR field requires that this slope be  $1/(n + 1)$ , which is 0.2 for 2024-0 aluminum. These plots indicate that the  $v$ -field exhibited a nearly LEFM field which later changed to an HRR field as the terminal load was approached. The  $u$ -field, on the other hand, exhibited an HRR field in the initial loading stage, but was quickly replaced by a non-linear zone at load exceeding 2600 ( N ). A similar trend was noted in the other three tests.

Figure 7 shows plots of the measured  $v$ - and  $u$ -displacements at a point of  $r = 1.2$  mm (1-1/2 plate thickness) and  $\theta = 45^\circ$ , where HRR field was shown to extend the furthest [8], with increasing applied load. Also shown are the corresponding  $u$ - and  $v$ -displacement fields for the LEFM and HRR fields at the same location. The displacements for the HRR field were calculated by using the average J-integral values obtained through contour integrations of the moire data. The corresponding displacement field for the LEFM crack tip were obtained by the equivalent plane-stress stress intensity factor computed from these J-integral values. A total of 34 numbers of log-log plots of the  $u$ - and  $v$ -fields were evaluated to arrive at the conclusion that only the  $v$ -field exhibited the HRR field through the loading and stable crack growth process.

The results are summarized in Figure 8 which shows the J-resistance curve of this 2024-0 specimen for  $B = 0$  and 2. Also shown are the approximate J-integral values, which were reported by Kang [12], for the same material but for a much smaller specimen. These J-resistance curves differ with others in that crack extension occurs at very low applied load and not due to blunting as reported by others [14]. Figure 9 shows the J-resistance values for 2024-T3 tests during stable crack growth. Also shown is the J-resistance curve obtained by de Koning [15] for a 2024-T3 center cracked panel with a thickness of 2-mm and Ernst [16] for 2024-T351 4T compact tension specimen. The major difference between the results of the two tests [15] is the knee, which occurred at the lower loads.

## DISCUSSION

The requirements for the J-dominance region for plane strain condition were discussed extensively in the articles by Hutchinson [17] and Shih [6]. This present discussion is limited to the analysis of HRR region of a moving crack in plane stress condition. Figure 7 showed that under the same loading, only the  $v$ -field exhibited the expected

progression from the LEFM to the HRR crack tip fields. At higher loading where the HRR singularity field should prevail, u-field does not show any HRR dominated region, but the v-field exhibited a prominent HRR field as shown in Figure 7. These results indicate that under rapid crack propagation, the desired HRR field may not exist in ductile materials and thus the dynamically modified J cannot be used as a far field parameter to characterize the ductile crack propagation.

#### CONCLUSIONS

- 1) HRR field exists only during initial loading for u-field and extended up to 2 mm from the crack tip.
- 2) HRR field exist in the v-field through the stable crack growth process and extended up to 10 mm from the crack tip.
- 3) J is path independent for crack extension of 5.6 mm for 2024-T3 and 2.2 mm for 2024-0 aluminum alloys.
- 4)  $J_R$  curves are identical within the scatter of data for 2024-T3 and 2024-0 for both  $B = 0$ ,  $B = 1$  and  $B = 2$ .

#### ACKNOWLEDGEMENT

This research was sponsored by the Office of Naval Research under ONR Contract No. N00014-85-K-0187. The authors wish to acknowledge the support and encouragement of Dr. Yapa Rajapakse, ONR, during the course of this investigation.

#### REFERENCES

1. J.R. Rice, ASME Journal of Applied Mechanics, 35 (1968), 379-386.
2. J.W. Hutchinson, Journal of the Mechanics and Physics of Solids, 16 (1968), 13-31.
3. J.R. Rice and G.F. Rosengren, Journal of the Mechanics and Physics of Solids, 16, (1968), 1-12.
4. R.M. McMeeking and D.M. Parks, Elastic-Plastic Fracture, ed. by J.D. Landes, J.A. Begley and G.A. Clarke, ASTM STP 668 (1979), 175-194.
5. C.F. Shih and M.D. German, International Journal of Fracture, 17 (1981), 27-43.
6. C.F. Shih, International Journal of Fracture, 29 (1985) 73-84.
7. C.F. Shih, R.G. deLorenzi and W.R. Andrews, Elastic-Plastic Fracture, ed. by J.D. Landes, J.A. Begley and G.A. Clarke, ASTM STP 668 (1979), 65-120.
8. F.P. Chiang and T.V. Hareesh, Proceeding of 1986 SEM Spring Conference on Experimental Mechanics, (1986), pp. 782-783.
9. J.S. Hawong, A.S. Kobayashi, M.S. Dadkhah, B.S.-J. Kang and M. Ramulu, Experimental Mechanics, 27 (1987) 146-153.

10. M.S. Dadkhah, F.X. Wang and A.S. Kobayashi, Experimental Techniques, 12 (1988), 28-30.
11. B.S.-J. Kang, A.S. Kobayashi and D. Post, Experimental Mechanics, 27 (1987) 234-245.
12. B.S.-J. Kang, A.S. Kobayashi, Experimental Mechanics, 28 (1988), pp. 154-158.
13. M.S. Dadkhah, A.S. Kobayashi, F.X. Wang and D.L. Graesser, Proceedings of the VI International Congress on Experimental Mechanics, (1988), pp. 227-234.
14. P.C. Paris, H. Tada, A. Zahoor, and H. Ernst, Elastic-Plastic Fracture, ed. by J.D. Landes, J.A. Begley and G.A. Clarke, ASTM STP 668 (1979), 5-36.
15. A.U. de Koning, Fracture 1977. Proceedings of the 4th International Conference on Fracture, Vol. 3A, Pergamon, (1978) 25-31.
16. H.A. Ernst, Scientific Paper 81-107-JINF-P6, Westinghouse R & D Center, Pittsburgh, Pa., Dec. 3, 1981.
17. J.W. Hutchinson, Journal of Applied Mechanics, 50 (1983), 1042-1051.

Accession For	
NTIS GRA&I	<input checked="" type="checkbox"/>
DTIC TAB	<input type="checkbox"/>
Unannounced	<input type="checkbox"/>
Justification	
By	
Distribution/	
Availability Codes	
Dist	Avail and/or Special
A-1	



Table 1 Test Matrix

Material Biaxial Load Ratio	2024-T3	2024-0
	Max. Crack Extension (mm)	
B = 0	3 MD031687	1.34 MD050288
B = 1	5.6 MD102687	—
B = 2	4 MD101987	2.2 MD050388

Table 2 J-integral Values Under Stable Crack Growth in  
2024-0 Aluminum Specimen MD050388, B ≈ 2.0.

Load in X (N)	Load in Y (N)	J (KPa-m)		Δa (mm)
		Contour 1	Contour 2	
2086	4066	4.0	3.8	0.14
2896	5489	11.0	10.5	0.6
3305	5591	18.1	18.4	0.85
3888	5845	31.0	29.0	1.37
3914	6076	32.0	29.2	1.4
4524	5720	34.0	31.0	1.68
4626	6810	50.0	47.0	2.2

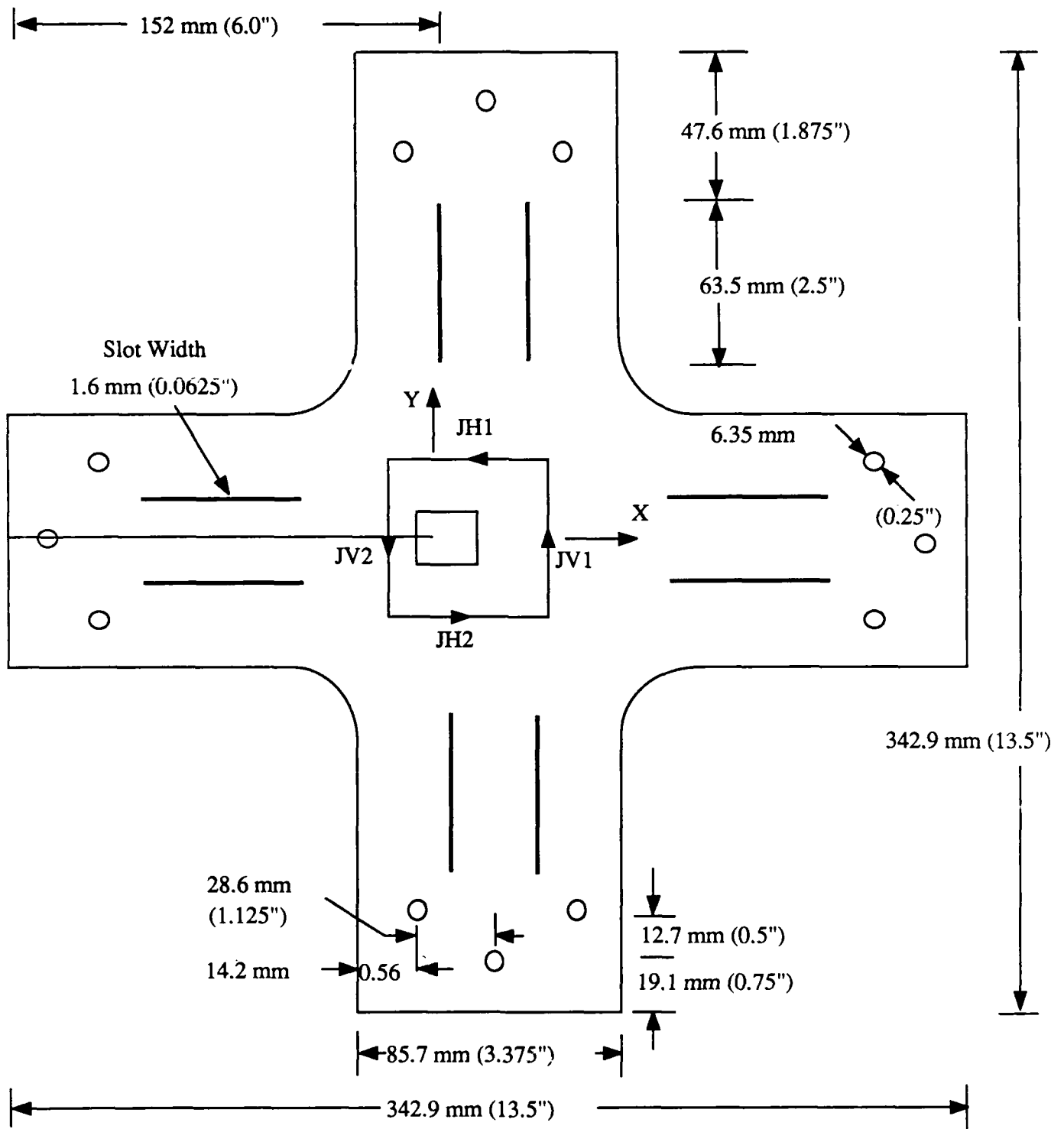


Figure 1 Specimen Configuration and J-integral Paths

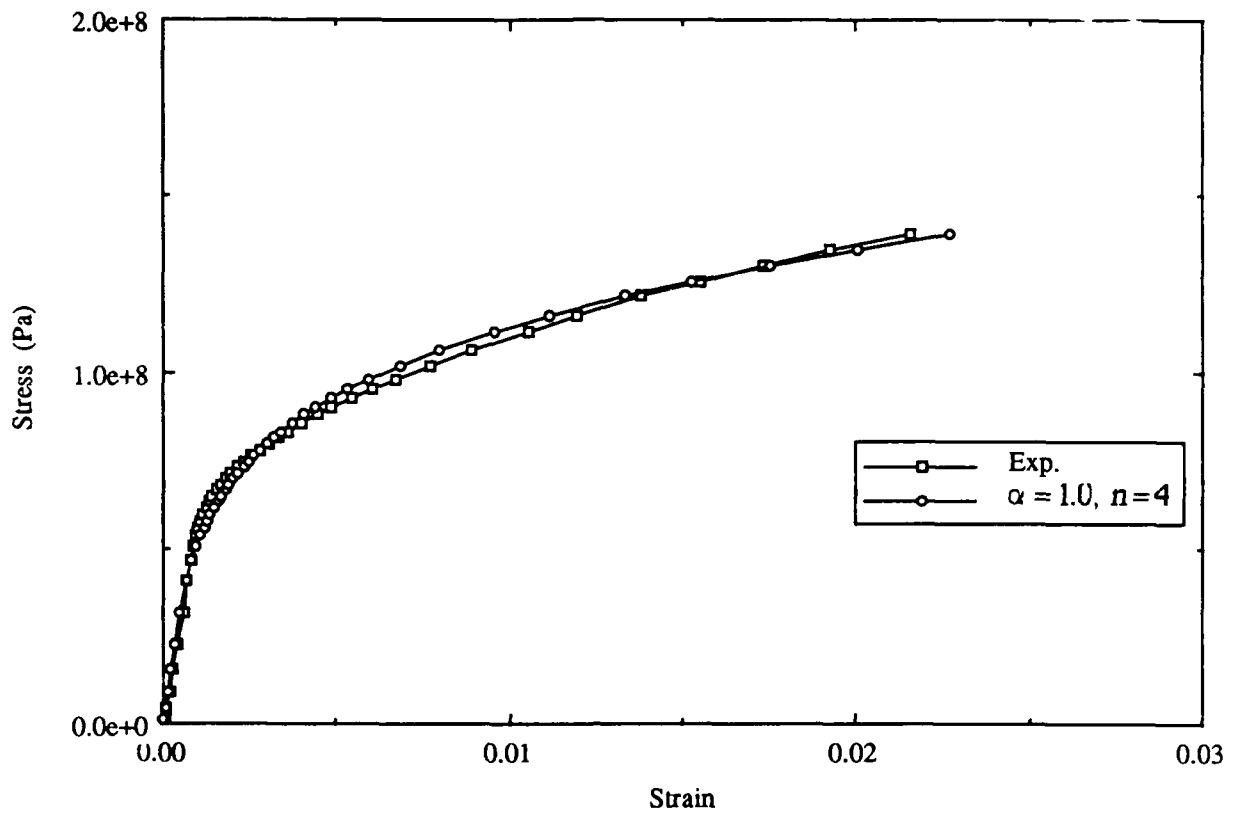


Figure 2a Uniaxial Stress-Strain Curve for 2024-0.

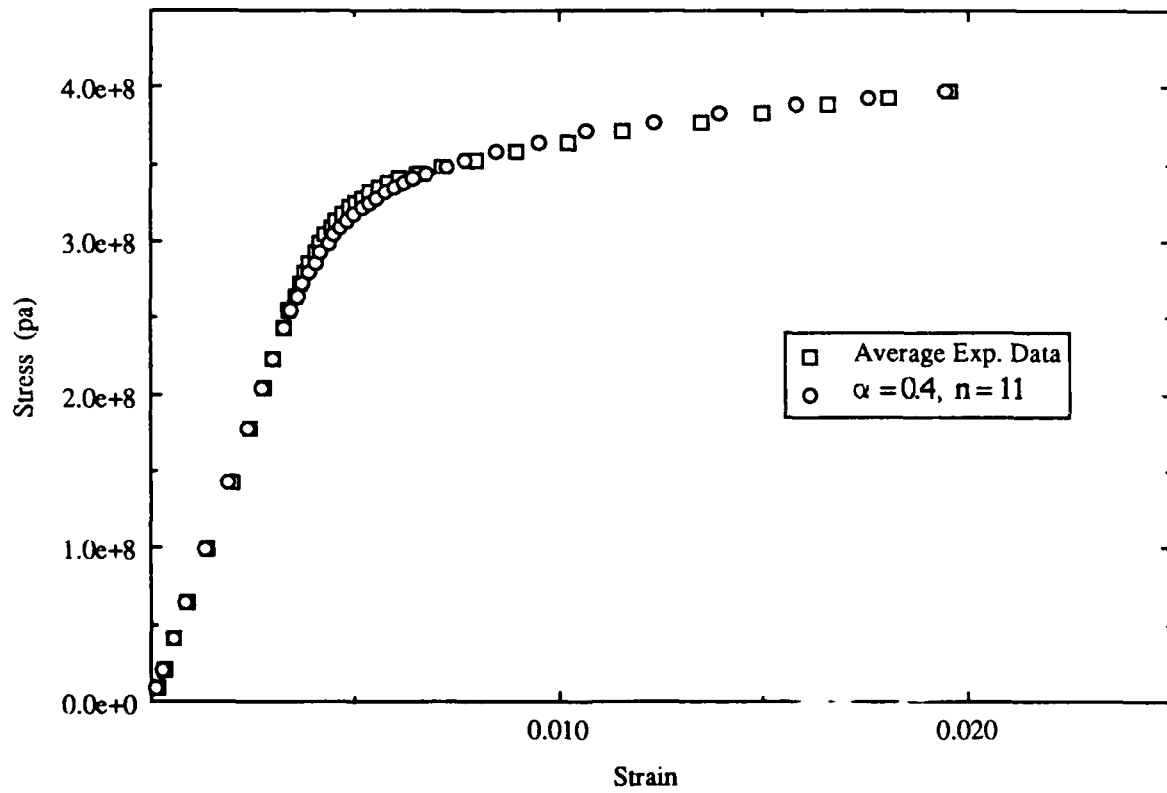


Figure 2b Uniaxial Stress-Strain Curve for 2024-T3.

"Load-Load Line Disp." MD050388

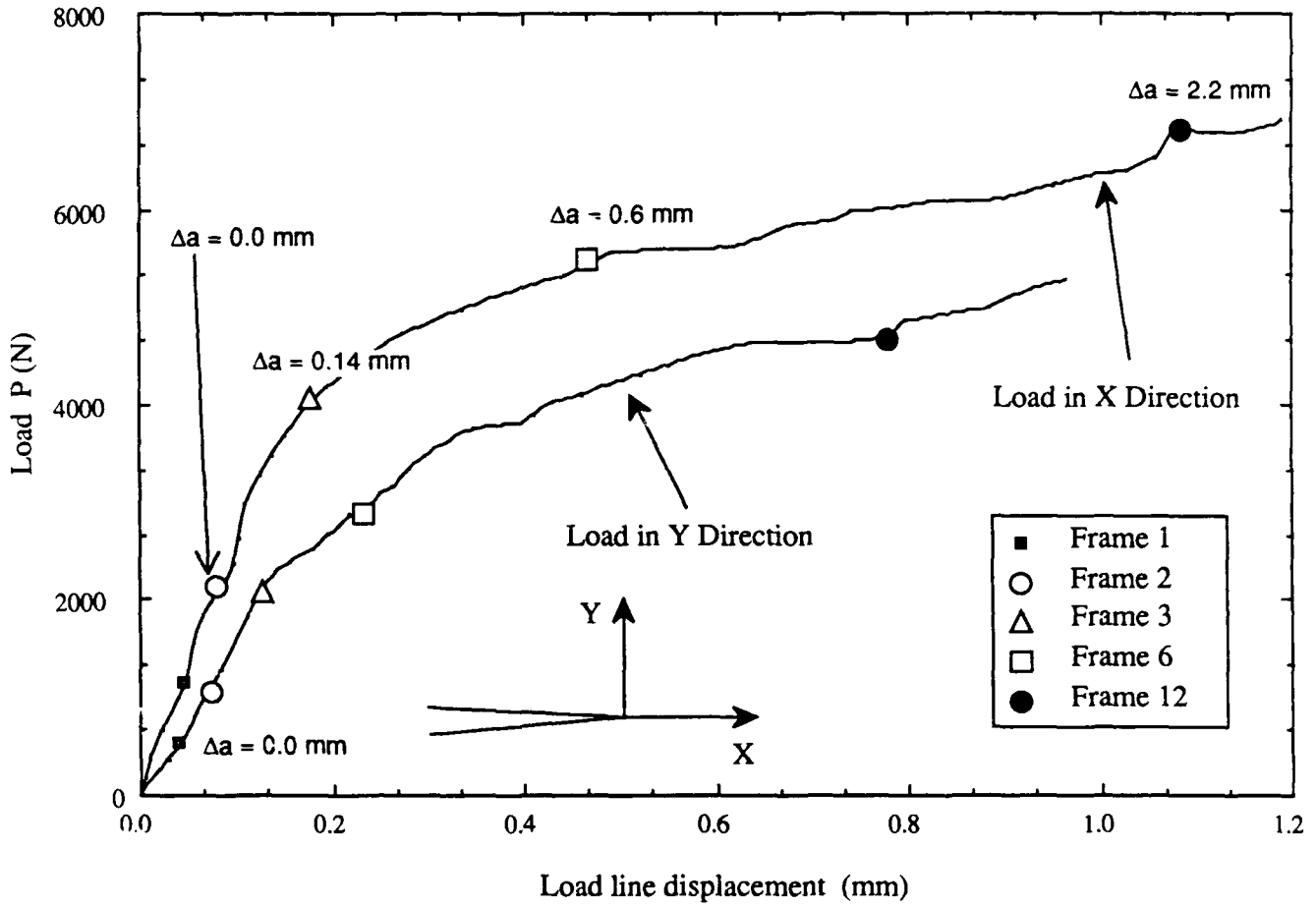


Figure 3 Load versus Load-line Displacement in 2024-0 Aluminum Specimen, B = 2.

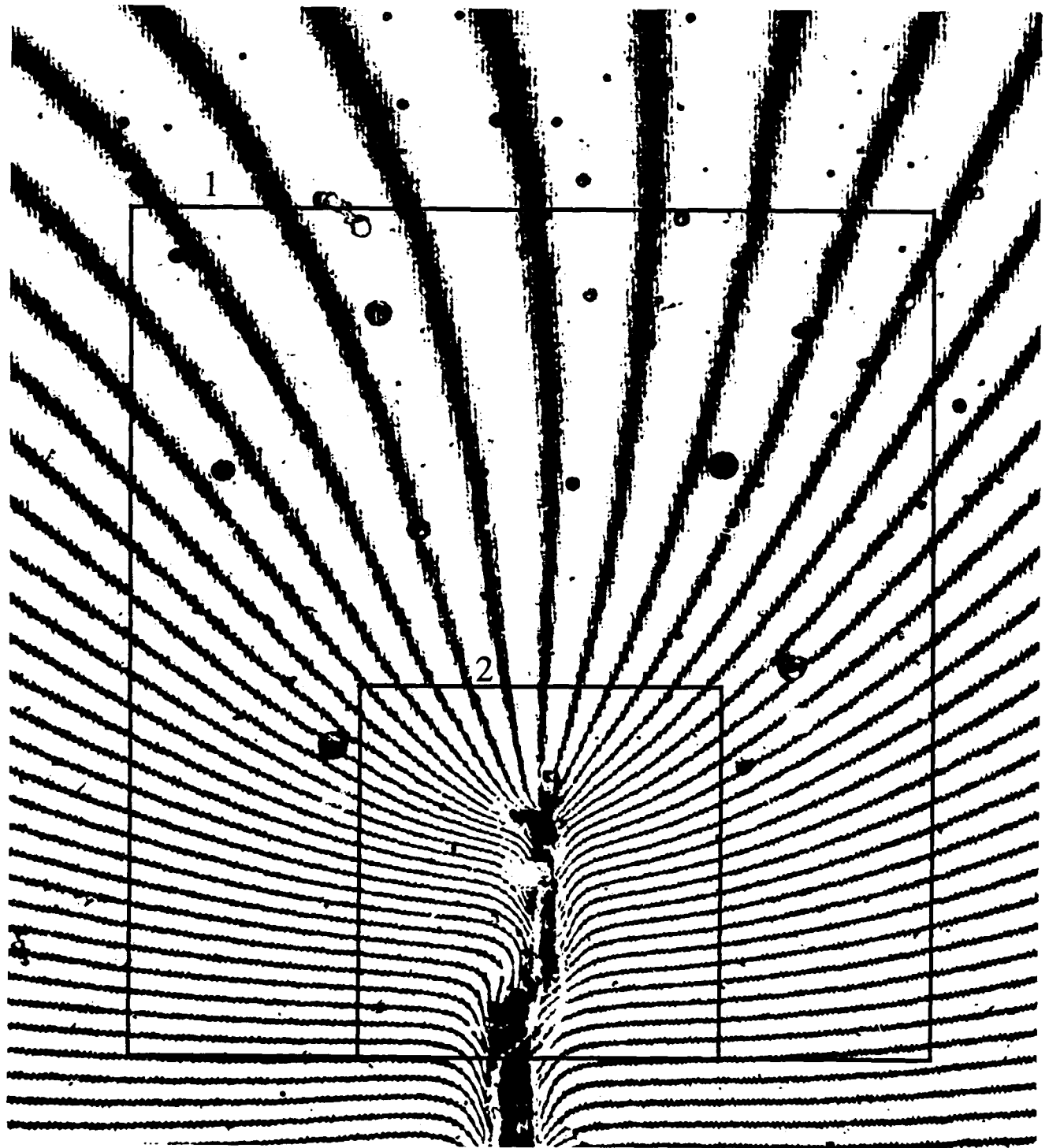


Figure 4a v-displacement in 2024-0 Aluminum Specimen, MD050388-3,  
 $B = 2.0$ ,  $\Delta a = 0.14$  (mm),  $F_x = 4066$  (N) and  $F_y = 2086$  (N).



5 mm

Figure 4b u-displacement in 2024-0 Aluminum Specimen, MD050388-3,  
 $B \approx 2.0$ ,  $\Delta a = 0.14$  (mm),  $F_x = 4066$  (N) and  $F_y = 2086$  (N).

Log(v)-Log(r) "MD050388V-3", 2024-0, B=2  
 Loads,  $F_x = 4066$  (N),  $F_y = 2086$  (N)  
 $a = 152$  (mm) + 2.7 (mm) Pre Fatigued  
 $\Delta a = 0.14$  (mm),  $n = 4$

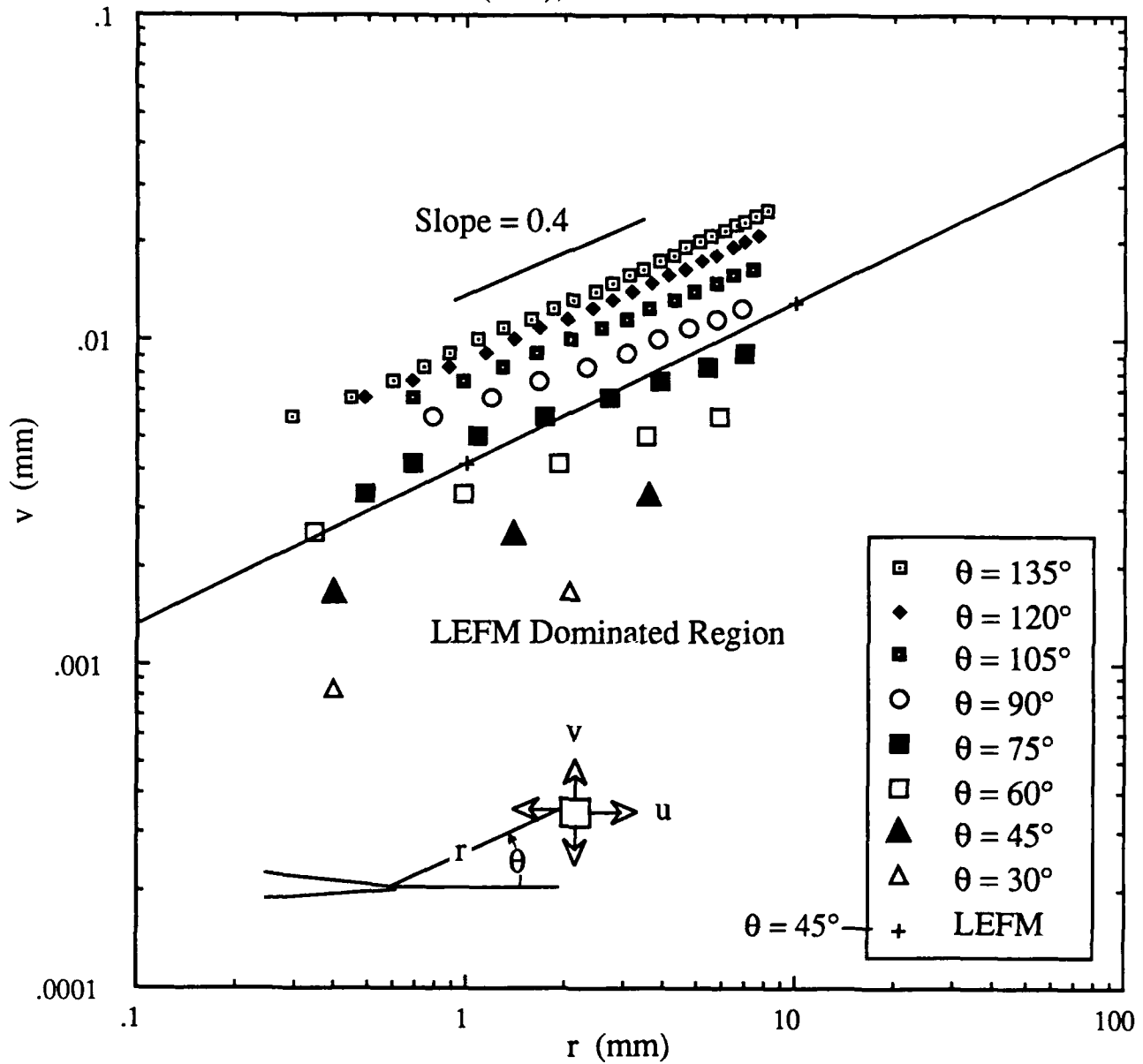


Figure 5a  $v$ -Displacement Versus  $r$  Relation for Various  $\theta$ , 2024-0 Aluminum MD050388-3  
 $B \approx 2.0$ ,  $\Delta a = 0.14$  mm,  $F_x = 4066$  (N) and  $F_y = 2086$  (N).

Log(u)-Log(r) "MD050388U-3", 2024-0, B=2  
 Loads  $F_x = 4066$  (N),  $F_y = 2086$  (N)  
 $a = 152$  (mm) + 2.7 (mm) Pre Fatigued  
 $\Delta a = 0.14$  (mm),  $n = 4$

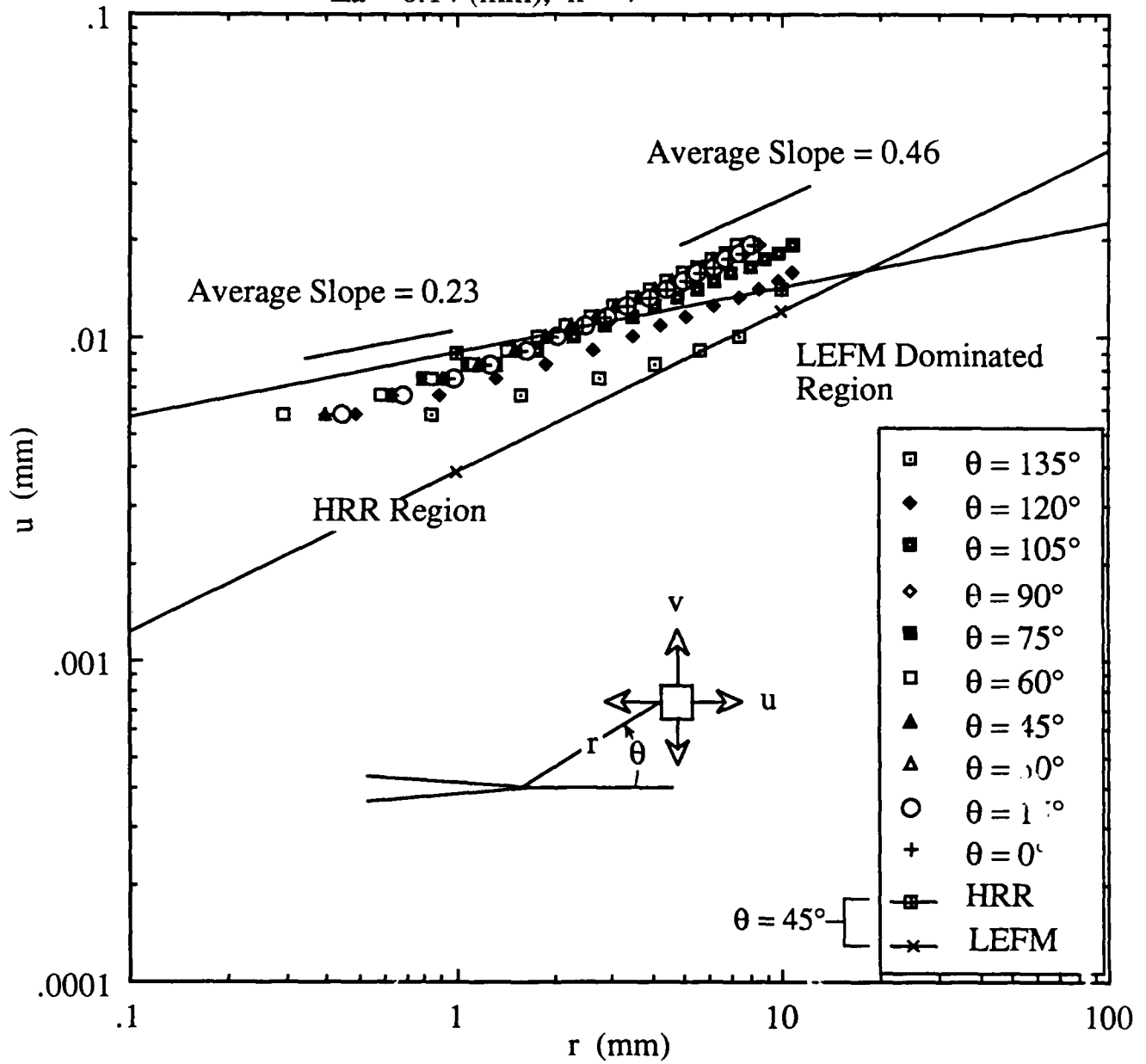


Figure 5b u-Displacement Versus r Relation for Various  $\theta$ , 2024-0 Aluminum MD050388-3  
 $B \approx 2.0$ ,  $\Delta a = 0.14$  mm,  $F_x = 4066$  (N) and  $F_y = 2086$  (N).

Log(v)-Log(r) "MD050388V-12", 2024-0  
 Loads,  $F_x = 6810$  (N),  $F_y = 4626$  (N)  
 $a = 152$  (mm) + 2.7 (mm) Pre Fatigued  
 $\Delta a = 2.2$  (mm),  $n = 4$

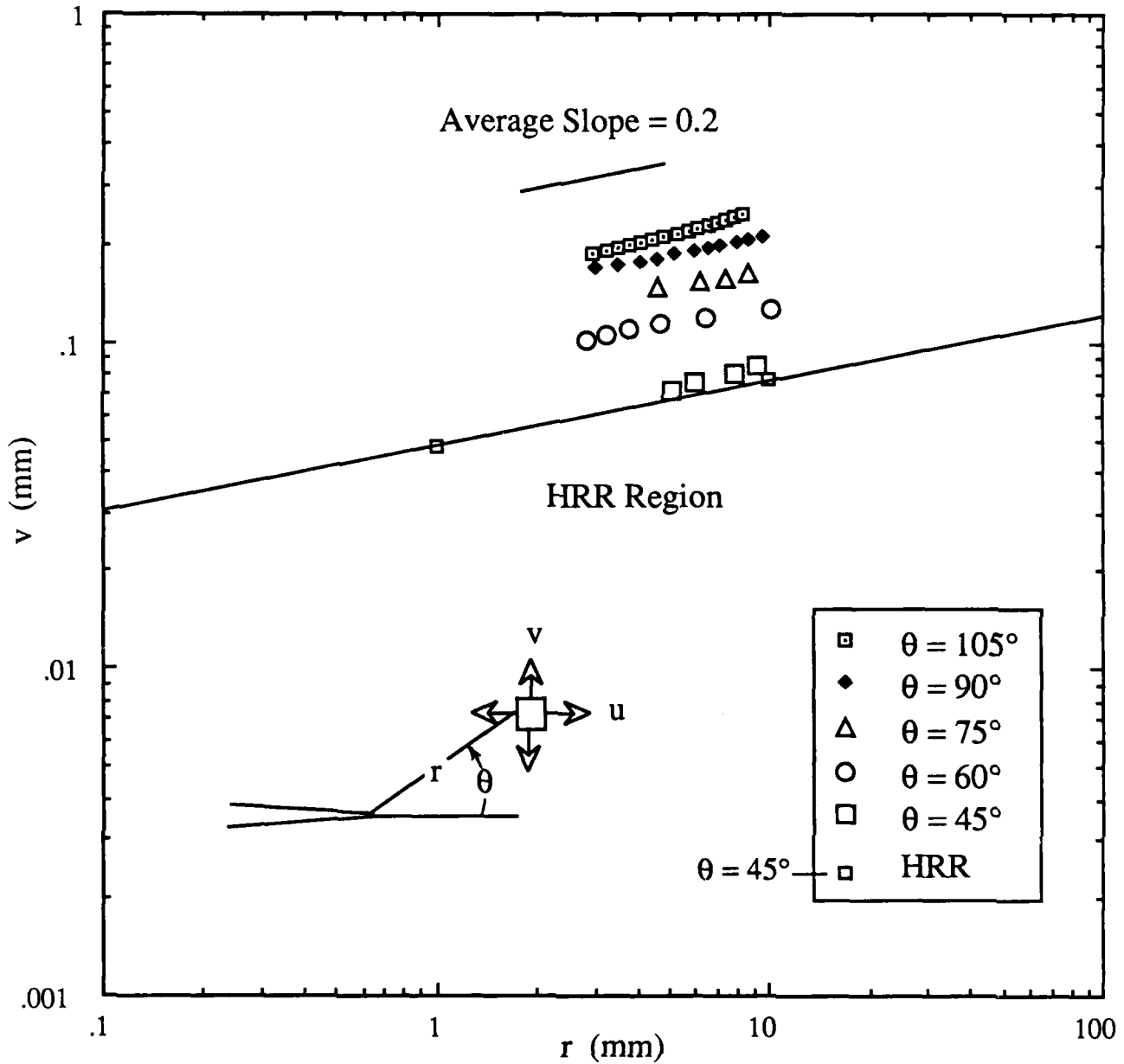


Figure 6a v-Displacement Versus r Relation for Various  $\theta$ , 2024-0 Aluminum MD050388-12  
 $B \approx 2.0$ ,  $\Delta a = 2.2$  mm,  $F_x = 6810$  (N) and  $F_y = 4624$  (N).

Log(u)-Log(r) "MD050388U-12", 2024-0  
 Loads,  $F_x = 6810$  (N),  $F_y = 4626$  (N)  
 $a = 152$  (mm) +  $2.7$  (mm) Pre Fatigued  
 $\Delta a = 2.2$  (mm),  $n = 4$

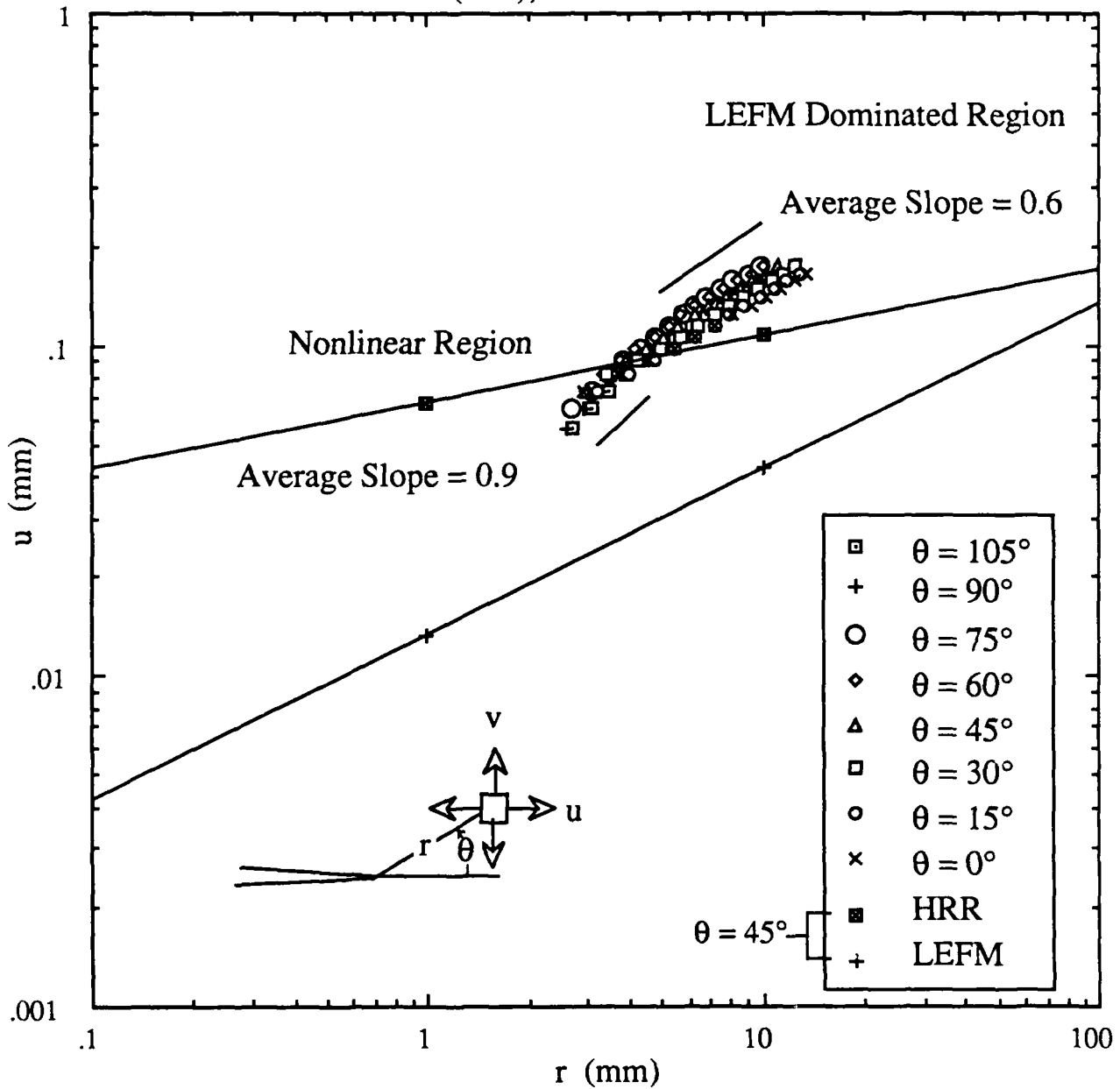


Figure 6b  $u$ -Displacement Versus  $r$  Relation for Various  $\theta$ , 2024-0 Aluminum MD050388-12  
 $B \approx 2.0$ ,  $\Delta a = 2.2$  mm,  $F_x = 6810$  (N) and  $F_y = 4624$  (N).

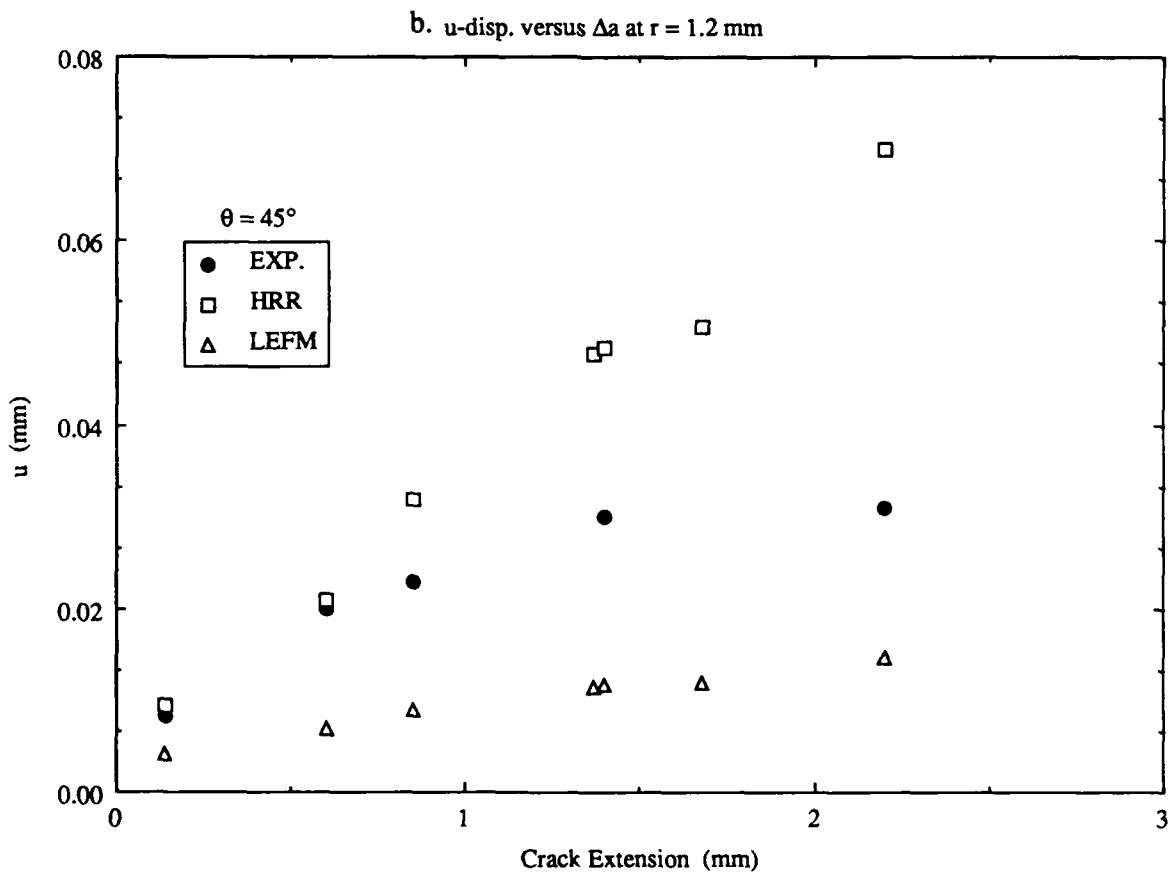
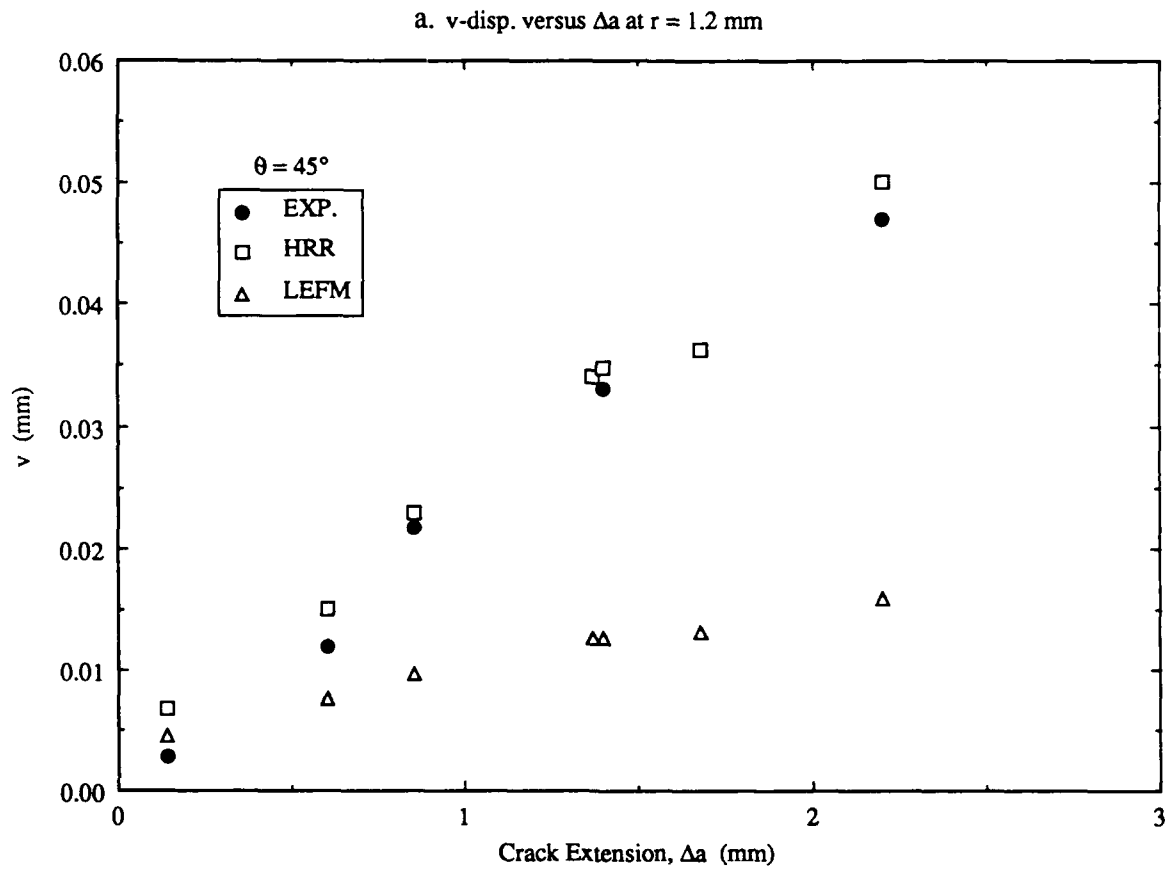


Figure 7 v- and u-Displacements at a point of  $r = 1.2$  mm and  $\theta = 45^\circ$  versus Crack Extension

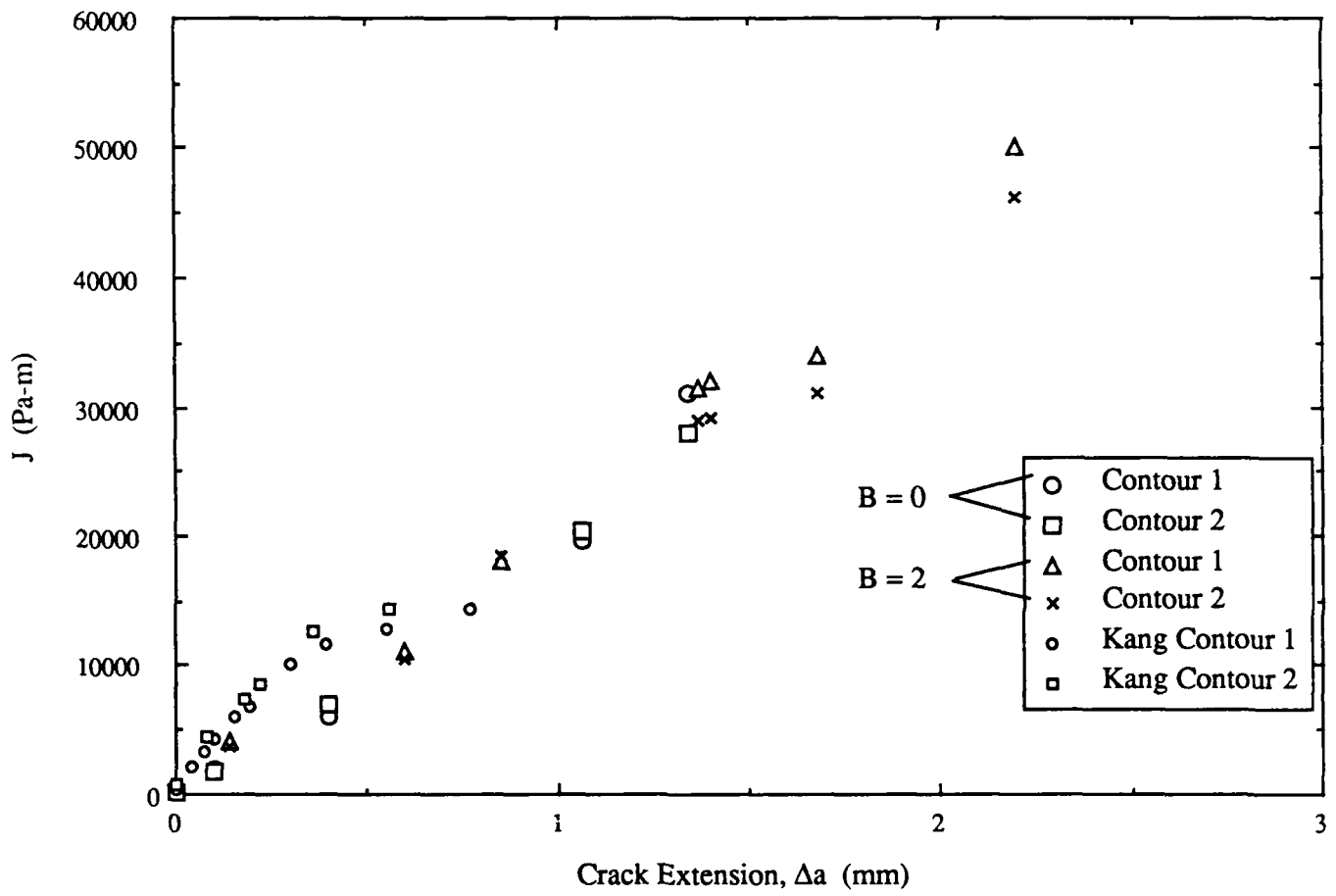


Figure 8  $J_R$  Curve of all 2024-0 Aluminum Tests.

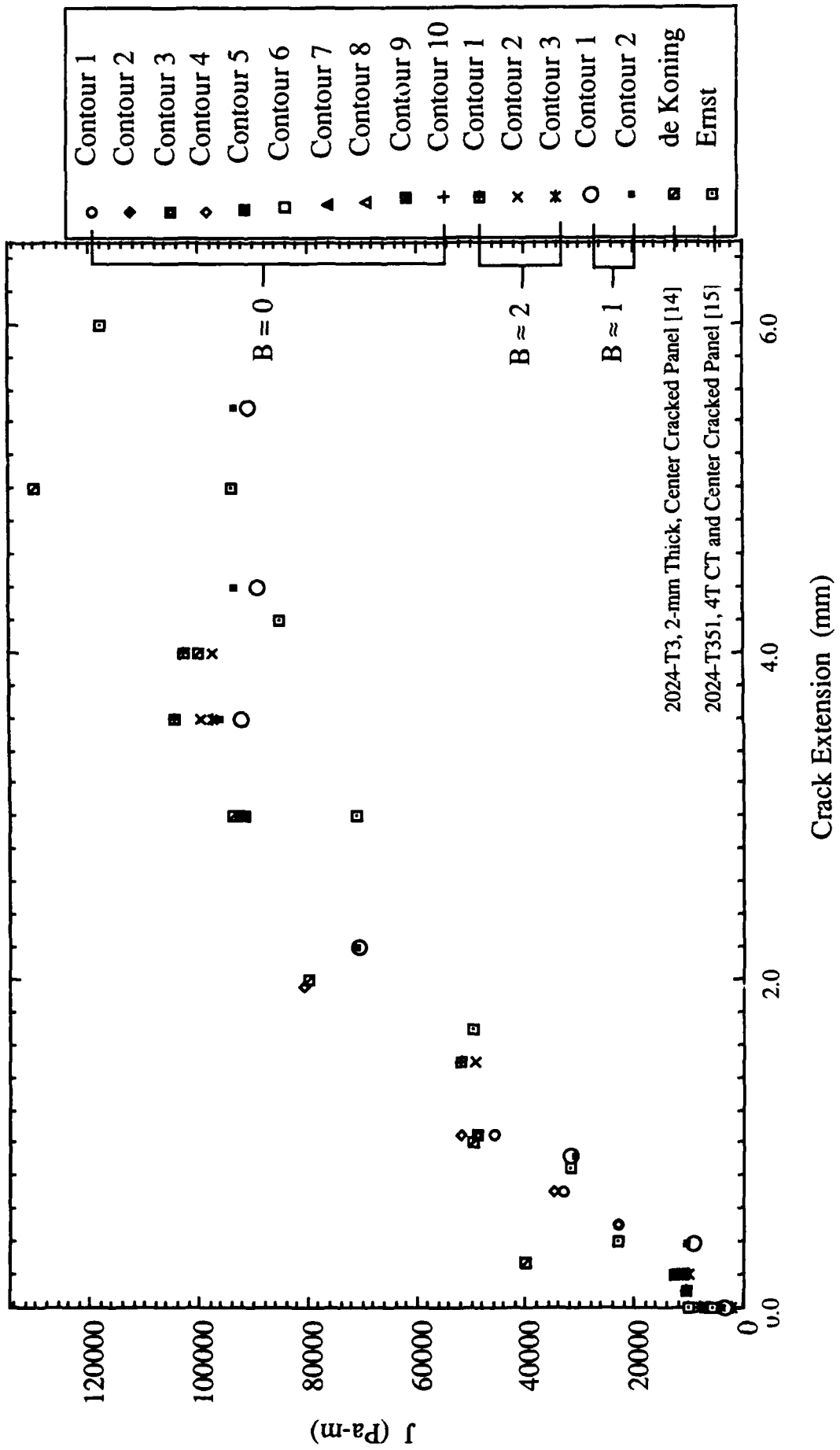


Figure 9  $J_R$  Curve for all 2024-T3 Aluminum Tests of this study, Ref. [14] and [15].

UNCLASSIFIED

SECURITY CLASSIFICATION OF THIS PAGE (When Date Entered)

A198931

REPORT DOCUMENTATION PAGE		READ INSTRUCTIONS BEFORE COMPLETING FORM
1. REPORT NUMBER UWA/DME/TR-88/60	2. GOVT ACCESSION NO.	3. RECIPIENT'S CATALOG NUMBER
4. TITLE (and Subtitle) HRR FIELD OF A MOVING CRACK, AN EXPERIMENTAL ANALYSIS		5. TYPE OF REPORT & PERIOD COVERED Technical Report
7. AUTHOR(S) M. S. DADKHAH, A. S. KOBAYASHI		6. PERFORMING ORG. REPORT NUMBER UWA/DME/TR-88/60
9. PERFORMING ORGANIZATION NAME ADDRESS Department of Mechanical Engineering, FU-10 University of Washington Seattle, Washington 98195		8. CONTRACT OR GRANT NUMBER(S) N00014-85-K-0187
11. CONTROLLING OFFICE NAME AND ADDRESS Office of the Chief of Naval Research Arlington, VA 22217-5000		10. PROGRAM ELEMENT, PROJECT, TASK AREA & WORK UNIT NUMBERS
14. MONITORING AGENCY NAME & ADDRESS (if different from Controlling Office)		12. REPORT DATE Sept. 1988
		13. NUMBER OF PAGES 18
		15. SECURITY CLASS. (of this report) Unclassified
		15a. DECLASSIFICATION/DOWNGRADING SCHEDULE
16. DISTRIBUTION STATEMENT (of this Report) Unlimited		
17. DISTRIBUTION STATEMENT (of the abstract entered in Block 20, if different from report)		
18. SUPPLEMENTARY NOTES		
19. KEY WORDS (Continue on reverse side if necessary and identify by block number) HRR Field, J-integral, Biaxial Loading, LEFM, Moiré Interferometry, Elastic-Plastic Fracture Mechanics, Simultaneous Displacement Fields, J-Dominance, J-resistance, Curve and Stable Crack Growth.		
20. ABSTRACT (Continue on reverse side if necessary and identify by block number) An improved moire interferometry was used to record simultaneously both the vertical and horizontal displacements associated with stable crack growth in uniaxially and biaxially loaded 2024-0 and 2024-T3 aluminum, single edge notched specimens. For stable crack growth up to 5 mm, the vertical displacement field showed the dominance of the HRR field but the HRR field was detected in the horizontal displacement only at the initial stage of loading. The far and near field J-integrals were path independent and yielded the correct crack tip displacements only at the initial stage of loading in the horizontal direction and at the terminal stage of loading in the vertical displacement field. The preliminary results indicate that J-characterization of a moving crack, including that of rapid propagation, may not be valid for these ductile materials for this specimen configuration.		

DD FORM 1473  
1 JAN 73EDITION OF 1 NOV 65 IS OBSOLETE  
S/N 0102-014-6601

UNCLASSIFIED

SECURITY CLASSIFICATION OF THIS PAGE (When Date Entered)